CHEMISTRY
A European Journal

A Journal of
ChemPubSoc Europe

Accepted Article

Title: Single-Crystal-to-Single-Crystal (SCSC) Linear Polymerization of a Desymmetrized Anthraphane

Authors: Marco Servalli, Nils Trapp, and Dieter Schlüter

To be cited as: *Chem. Eur. J.* 10.1002/chem.201802513

Link to VoR: http://dx.doi.org/10.1002/chem.201802513

Supported by
ACES

WILEY-VCH

10.1002/chem.201802513

WILEY-VCH

FULL PAPER

Single-Crystal-to-Single-Crystal (SCSC) Linear Polymerization of a Desymmetrized Anthraphane

Marco Servalli*[a], Nils Trapp[b], A. Dieter Schlüter[c]

Abstract: In this work we present one of the rare cases of single-crystal-to-single-crystal (SCSC) linear polymerizations, resulting in a novel ladder-type polymer. The polymerization is based on the photoinduced [4+4]-cycloaddition reactions between trifunctional anthracene-based monomers. The careful design of the monomer anthraphane-tri(OMe), results in perfectly stacked anthracene pairs in the crystal structure, with Schmidt's distances *d* = 3.505-3.666 Å and shift *s* = 1.109 Å, allowing a selective linear polymerization in quantitative yields and in a matter of minutes, without compromising the integrity of the single crystals. The obtained polyanthraphane-tri(OMe), reveals moreover a very interesting and unprecedented case of stereoisomerism, which is characteristic for polyanthraphanes.

Introduction

Anthraphane **1** is a novel D_{3h}-symmetric hydrocarbon cyclophane equipped with three photoreactive anthracene units designed for topochemical reactions in single crystals[1–4] (Figure 1). The reactions are brought about by photochemical [4+4]-cycloadditions between face-to-face (*ftf*) stacked anthracene pairs[5–8]. Compound **1** is particularly interesting because its three equally reactive sites cause a unique potential versatility in terms of solid state reactivity. It can not only afford dimers and linear ladder polymers[9,10], but also two-dimensional polymers[11–13] can be envisaged, depending on how the anthracene units are arranged in the crystal structure and whether one, two or even three of these units involve themselves in dimerization reactions. We therefore started a research program initially concentrating on the study of the crystallization and packing behavior of parent anthraphane **1**. Seven main packing motifs were found, three of which photoreactive[14]. They gave either the dimer dianthraphane or a novel linear polymer, the poly$_{1D}$anthraphane, **PA1**, in quantitative yields and in a single-crystal-to-single-crystal (SCSC) fashion[15]. Topochemical polymerizations have long been reported[16–22] together with SCSC reactions[23,24], however topochemical linear polymerization which proceed in a SCSC fashion resulting in covalent polymers are still a rarity in the literature[15,25–29]. Encouraged by the rich and highly selective photoreactivity of compound **1**, we are currently widening our activities towards simple derivatives of the parent compound, whereby structural modifications are being considered which could have a direct influence on the geometry of anthracene pairs in the crystal structure. This way it was hoped to find new packing motifs that could help to widen the product diversity of anthraphanes in their SCSC reactions.

By analyzing the packings of parent compound **1** it became evident that the molecules had a tendency to interdigitate in the crystal structure, often resulting in anthracenes pairs slightly or completely laterally off-set, pushed closer than necessary to the central benzene rings of the respective other monomer. The observed offsets not only rendered some packings unreactive, but they also affected considerably the rate of photodimerization in reactive packings. We thought that this offsets could be sterically counteracted by introducing small groups to at least one of the central benzene rings of **1**. For symmetry reasons and synthetic feasibility considerations, three of these groups were envisaged, resulting in the design of anthraphane-tri(OMe), **2** (Figure 1). In this work, we present the facile synthesis of anthraphane **2** and disclose two new packing motifs (*etf* packing 3 and *etf*/*ftf* packing 5) this compound assumes in the single crystal, one of which being a particular case of polymorphism and also being reactive, furnishing in a SCSC fashion the novel linear ladder polymer poly$_{1D}$anthraphane-tri(OMe) **PA2**. Interestingly, not only do the main structural skeletons of **PA1** and **PA2** differ considerably, but it also appears that the methoxy substituents play a key role in the polymerization. In contrast to **PA1**, which passed through an intermediate dimer state, the crystal packing of monomer **2** allows for a better overlap in the anthracene pairs and, thus, for a higher polymerization reactivity. Intermediate states are not observed and photopolymerization proceeds smoothly in a matter of minutes.

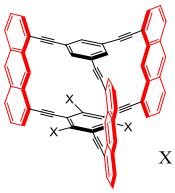

X = **1**, H **(previous study)**
2, OMe **(this work)**

Figure 1. Chemical structure of anthraphane **1** and its desymmetrized counterpart anthraphane-tri(OMe) **2** synthesized in this study.

[a] Dr. M. Servalli
Department of Materials
ETH Zurich
Vladimir-Prelog-Weg 5, 8093 Zurich (Switzerland)
E-mail: marcosendymion@gmail.com
[b] Dr. N. Trapp
Small Molecule Crystallography Center (SMoCC)
Department of Chemistry and Applied Biosciences
ETH Zurich
Vladimir-Prelog-Weg 1, 8093 Zurich (Switzerland)
[c] Prof. Dr. A. D. Schlüter
Department of Materials
ETH Zurich
Vladimir-Prelog-Weg 5, 8093 Zurich (Switzerland)

Supporting information for this article is given via a link at the end of the document.((Please delete this text if not appropriate))

10.1002/chem.201802513

Results and Discussion

Synthesis of anthraphane-tri(OMe)

It was desirable to introduce subsituents on the triethynylbenzene moiety that did not involve dramatic changes to the original synthetic protocol developped for anthraphane **1**[4]. As such, methoxy groups were chosen, due to their compatibility with the desylilation step and the basic conditions of the required Sonogashira reactions (Scheme 1). In particular, small substituents were also desirable to not sterically interfere with the final copper-free Sonogashira cross-coupling between the hexa-substituted benzene **6** and **8**. Moreover, to suppress the offset in the anthracene pairs in the crystals, simple model considerations suggested the methoxy substituents in compound **2** to be suitable.

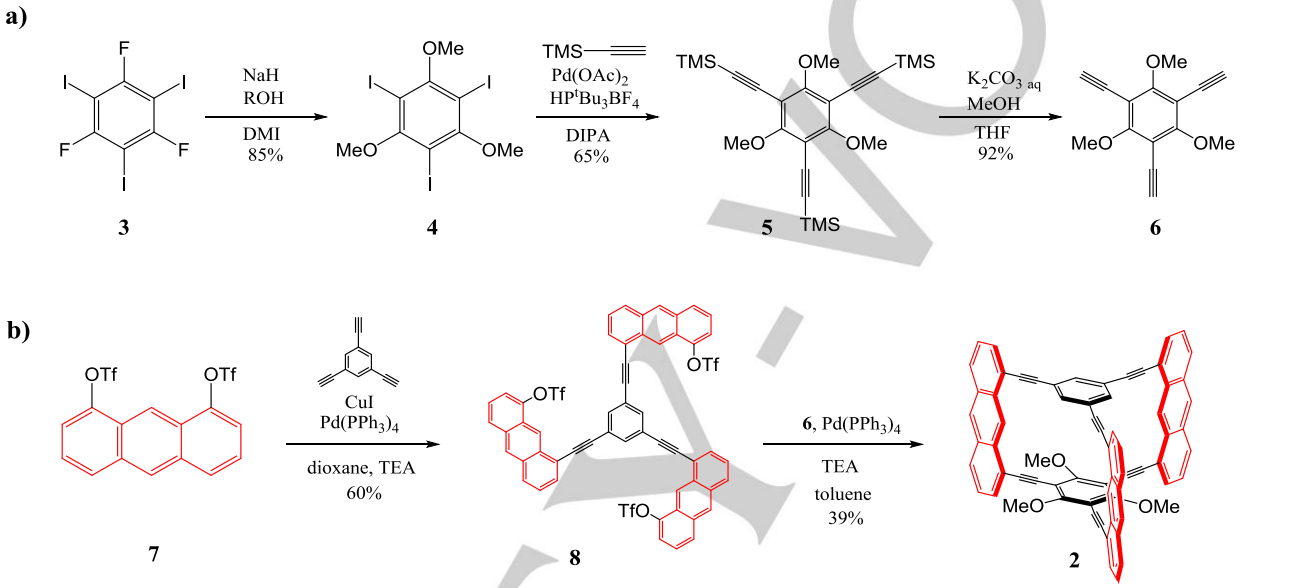

Scheme 1. Synthesis of the new anthraphane **2**. a) Route for the synthesis of the methoxy-substituted triethynylbenzene **6**, the key building block required in the last step. b) Sequential Sonogashira cross-coupling reactions of ditriflate **7** with the triethynylbenzene core and of the resulting tritriflate **8** with the substituted triethynylbenzene core **6** from route a).

The synthesis of the trimethoxy-substituted benzene core **6** was adapted and modified from an already published procedure from Hennrich[30,31] (Scheme 1a): in a first step, 1,3,5-trifluorobenzene was quantitatively iodinated with periodic acid in sulfuric acid to give compound **3**[32]. Triple nucleophilic aromatic substitution of the fluorides in anhydrous DMI with freshly prepared sodium methoxide yielded the methoxy-substituted iodinated compound **4** in 85% yield**.** For the Sonogashira cross-coupling of **4** with trimethylsilylacetylene, the reaction conditions were slightly changed due to the particularly poor reactivity of **4** towards oxidative addition[33]. Instead of the standard $Pd(PPh_3)_4$, the more aggressive and nucleophilic catalyst $Pd(P^tBu_3)_2$ was used[34], which was generated in situ from $Pd(OAc)_2$ and by deprotonation of $HP^tBu_3BF_4$ with DIPA. For such an electron-rich substrate, the reaction worked very well with yields up to 65%. In a final step, desylilation of **5** with potassium carbonate in methanol afforded quantitatively the target compound **6** in high purity.

With the substituted core in hand, **2** was then assembled by using the same conditions employed for the synthesis of anthraphane (Scheme 1b). Conveniently, the final step worked as nicely as in the original synthesis and the work-up to isolate the monomer did not have to be changed: from 640 mg of precursor **8**, 203 mg of **2** were obtained in 39% yield in form of an amorphous powder. The structure of anthraphane-tri(OMe) **2** was unambiguously confirmed by ^{1}H-NMR and ^{13}C-NMR spectroscopy, high-resolution mass spectrometry and by SC-XRD.

Crystallization of 2 and its packings in the single crystal

Desymmetrization of anthraphane **1** to compound **2** involved addition of three methoxy groups and thus a reduction of symmetry from D_{3h} to the C_{3v} point group; as such, an increase in solubility was expected, which in fact was observed and allowed to measure a fully resolved ^{13}C-NMR spectrum in solution (Figure S5). The best crystallization method was slow cooling of nearly saturated solutions. The solvents employed were THF, dioxane, chloroform, 1-methylnaphthalene and nitrobenzene. The amorphous powder obtained from the work-up was suspended in the desired solvent, which was then heated close to the boiling point until a clear solution was obtained. This solution was then cooled to room temperature over 24 h (for details see page S14 in the SI). Single crystals were obtained in all cases and analyzed by SC-XRD: three main packing motifs were obtained, summarized in Figure 2.

10.1002/chem.201802513

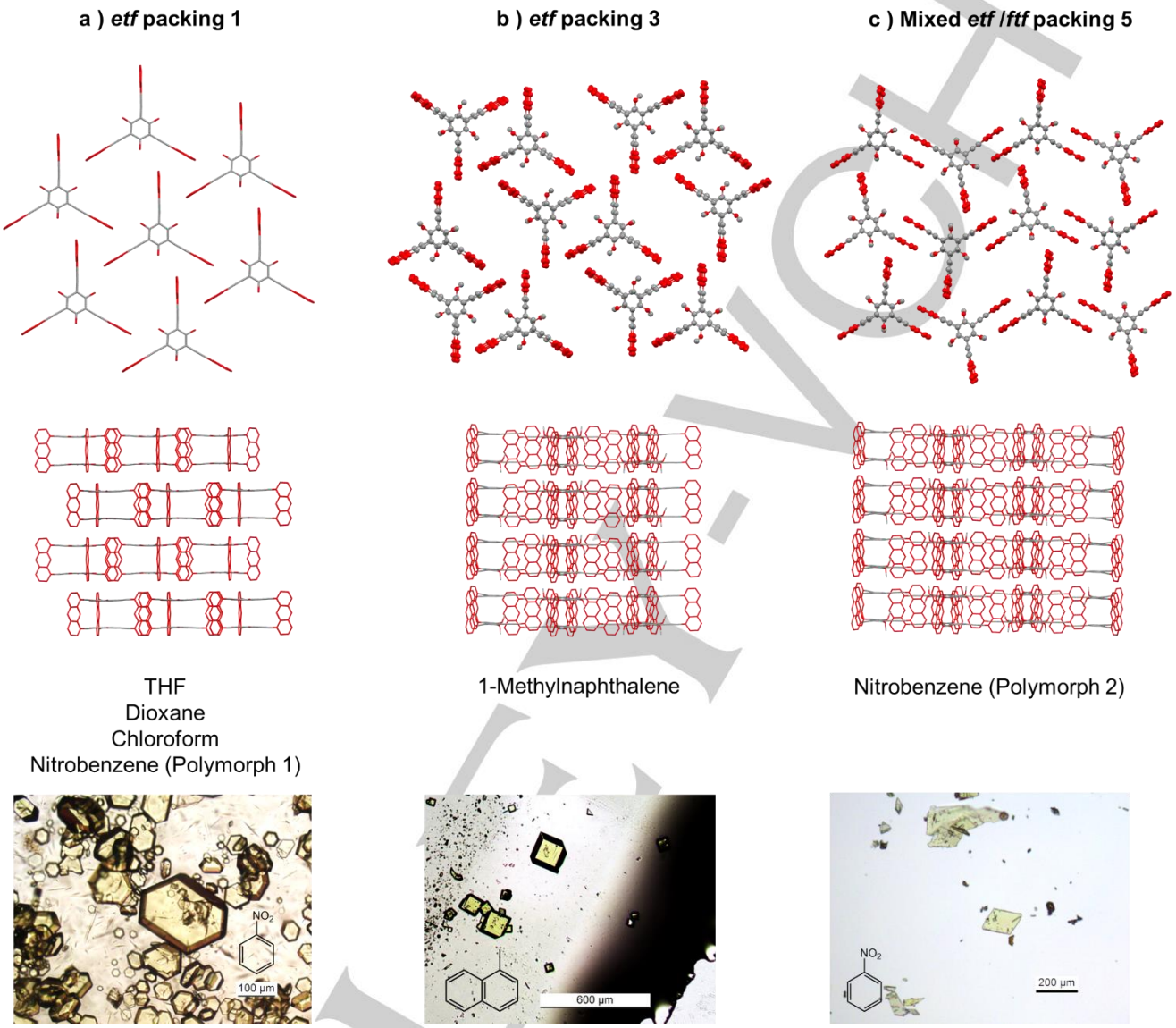

Figure 2. The three packing motifs obtained for compound **2**: a) *etf* packing 1, b) *etf* packing 3 and c) mixed *etf/ftf* packing 5. The same packing nomenclature from the hydrocarbon anthraphane **1** was used[14]. From *top* to *bottom*: top view of a layer in the crystal structures, layer arrangement in the crystal structure, solvents from which the packing can be obtained, optical micrograph of representative single crystals. The photoreactive anthracene units are colored in red, solvent molecules are omitted for clarity. Please note that the displayed *etf* packing 1 motif is based only on a fragmentary structure solution due to excessive disorder in the crystals (see text); for that reason the model is represented as "capped sticks" and the methyl groups were omitted. The *etf* packing 3 and *etf/ftf* packing 5 are instead real crystal structures.

Before going into an analysis of the three different packing motifs obtained, a comment concerning crystal quality is appropriate. In particular all the crystals belonging to the *etf* packing 1 had a high degree of disorder both in the main molecule and solvent molecules incorporated in the structure, preventing fully resolved X-ray structure analysis. The packing displayed in Figure 2a is based on fragmentary structure solution only and should not be regarded as a real and complete crystal structure; despite the fragmentary solution however, the edge-to-face motif however could be clearly discerned. The packings displayed in Figure 2b and 2c correspond instead to real and solved crystal structures.

The *etf* packing 1 (the nomenclature of the packing motifs was kept from reference [14]) was obtained from THF, dioxane and chloroform in the form of yellow needles. Hexagonal plates were instead obtained from nitrobenzene in a case of polymorphism (see below). In this packing all the anthracene units are arranged in an edge-to-face fashion and cannot therefore photoreact. This packing motif was also a very common

10.1002/chem.201802513

occurrence for the parent hydrocarbon anthraphane **1** and we were therefore not surprised by the outcome. As indicated before, the desymmetrized **2** in this packing always resulted in poor quality crystals, in which the molecule intrinsically does not seem to have a preferred orientation: while it always packs in layers, in each layer some molecules have the substituted core oriented in one direction and some in the opposite direction. While the *etf* motifs were clearly discernible, the reliability factors always resulted too high for an acceptable structural model. Crystals from this packing were also very sensitive upon manipulation, easily losing solvent when taken out of their mother liquor and completely losing crystallinity when rinsed with other solvents. This is likely due to the porous nature of this packing. Using slow vapor diffusion as crystallization method did not yield better quality crystals.

Better results were obtained by using 1-methylnaphthalene as crystallization solvent: yellow cubes were obtained and upon SC-XRD analysis, a new packing motif was discovered, the *etf* packing 3 (Figure 2b). As the name suggests, in this packing there is again an exclusive edge-to-face relationship between the anthracene units of **2**. There are parallel anthracene units in the structure but they are too offset to be photoreactive. The voids between the molecules are filled by solvent molecules; two methylnaphthalene molecules are π-π stacking with each other (for more detail see Figure S11). The overall structure can be regarded as arrays of cyclophanes arranged in layers and held together by solvent molecules and a large parallel displaced π-π stacking interaction between anthracene moieties. Molecules in arrays are stacked on top of each other and have a preferred orientation of their trimethoxybenzene moieties: between neighboring arrays the orientation alternates itself (Figure S12). This is the only structure in this study in which the trimethoxy-benzene units of the molecules have a clear preferred orientation.

Crystallization from nitrobenzene afforded yellow rhombohedral plates which upon SC-XRD analysis also resulted in a new packing motif: *etf*/*ftf* packing 5 (Figure 2c). In this packing motif, each molecule has two anthracene units face-to-face stacking with the anthracene units of its neighbors, potentially leading to linear polymer chains upon photoreaction. The molecules again are packed in layers and the void between them are filled with nitrobenzene molecules (Figure S15). Two nitrobenzenes are π-π stacking with each other and with the third anthracene blade not involved in *ftf* stacking. These solvent molecules are disordered in their orientation, trying to avoid contact with the methoxy groups: the two orientations have roughly 80 : 20 occupation. This is a consequence of the main molecule also being disordered: from this it can be concluded that in average, in the crystal structure 80% of the cyclophanes have the trimethoxy-benzene rings oriented on one side and the remaining 20% oriented on the opposite side.

An interesting case of polymorphism was discovered when handling this nitrobenzene solvate: in an attempt to increase the quality of the single crystals from the first crystallization batch, we decided to recrystallize them again from nitrobenzene. After the second crystallization however, hexagonal platelets were obtained which surprisingly corresponded to the *etf* packing 1 (Figure S7). It can be reasoned that the small impurities present in the amorphous powder obtained after the synthetic workup are responsible for obtaining the photoreactive *etf*/*ftf* packing 5; in fact this result could be reproduced from three different batches of **2**. Removing the impurities by recrystallizing a second time results instead in the non-reactive packing. However, by recrystallizing the hexagonal platelets of the *etf* packing 1 and seeding the obtained clear solution with a rhombohedral single crystal from the first crystallization step, the photoreactive *etf*/*ftf* packing 5 could be obtained again selectively. It is noteworthy that these single crystals can be rinsed with methanol and dried without losing crystallinity; after one month stored in a vial they could be again measured by SC-XRD. Having the photoreactive crystals in hand, we then proceeded to investigate their photoreactivity.

Structural analysis and SCSC Photopolymerisation of 2

Crucial for a topochemical SCSC reaction is that the reactive units are in close proximity and properly aligned and oriented in the crystal structure. In the case of anthracene pairs, they have to *ftf*-stack properly with good overlapping between the p-orbitals at their reactive 9, 10 positions. A geometrical analysis of the anthracene pairs can help to assess their photoreactivity: useful parameters are the distance between the respective C9 and C10 positions $d_{9,10'}$ and $d_{10,9'}$ (the so-called Schmidt's distances[35]) and the shift *s*, which describes the planar shift of the anthracene rings' centroids from an ideally coplanar superimposed anthracene pair and is therefore a measure of the overall offset of the pair. Since the two anthracene units of **2** are *ftf*-stacking equivalently in the crystal structure, only one pair is displayed in Figure 3a. The anthracenes are not exactly coplanar having a plane angle of approximately 3°; consequently two different distances $d_{9,10'}$ and $d_{10,9'}$ are present, 3.666 Å and 3.505 Å. The shift value *s* accounts for roughly 1.109 Å, corresponding to a minor offset in the pair. These values suggest a stacking particularly suitable for a SCSC photoreaction. Compared to the previous study on **1** and the resulting polymer **PA1**, the geometrical parameters of **2** are much better: for **1**, *d* values were ranging from 3.695 – 3.948 Å and shift values from 1.354 – 1.904 Å, above which reactivity was not observed[15]. High values were in fact shown to dramatically influence the SCSC reaction kinetics, by slowing down the reactivity of poorly overlapped pairs and consequently causing cracks in the crystals during the reaction, due to the pronounced molecular movement necessary for the pairs to better overlap and dimerize. In the current case we therefore expected a smooth and fast SCSC photopolymerisation, without having to pay too much attention to the irradiation conditions, such as temperature and time.

10.1002/chem.201802513

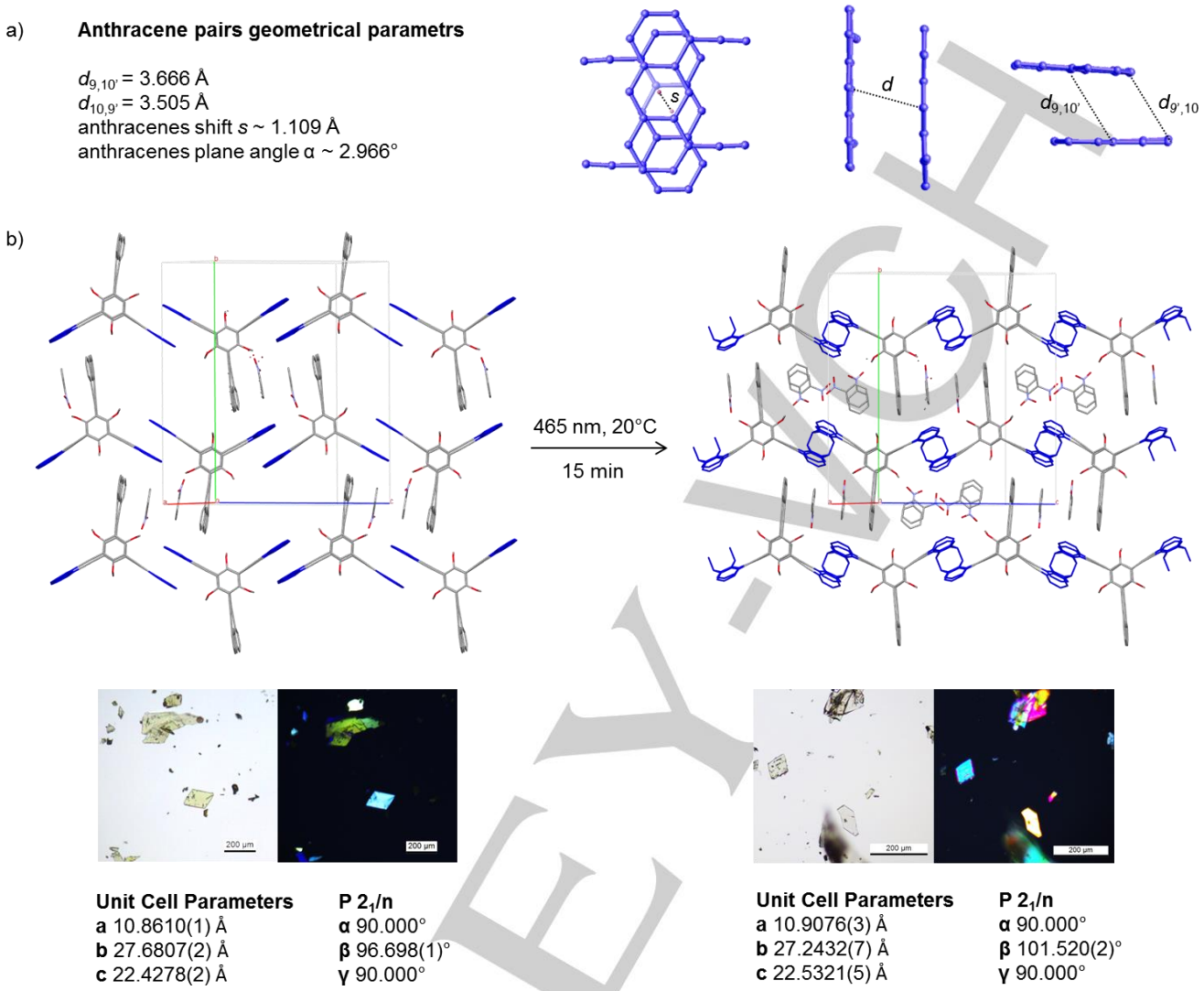

Figure 3. a) Geometrical parameters of the stacked anthracene pairs used to assess the photoreactivity; b) one-step SCSC linear photopolymerization of the nitrobenzene solvate in the *etf*/*ftf* packing 5. The reaction proceeds with minimal mismatches between the unit cell parameters of the monomer crystal and the polymer crystal, resulting in a smooth and fast polymerization at room temperature. Optical micrographs of the single crystals before and after polymerization are displayed in bright field mode and between crossed polarizers. Consumption of the anthracene units during polymerization results in crystal discoloration.

It is perhaps noteworthy to mention the cause of the nice stacking of the pairs of **2**: in our previous crystallization studies of **1** it was found in certain packings that the molecules had the tendency to interpenetrate resulting in offset anthracene pairs. Interpenetration can go as far as the hydrogen atoms of the central benzene cores start to sterically repel with the hydrogen atoms of the anthracene edge. In **2** instead, the substitution of the hydrogen atoms of the central benzene core with methoxy groups prevents interdigitation resulting in nicely stacked anthracene pairs (Figure 4). This appears like an interesting element of crystal engineering[36,37] which could be applied in the future for this kind of molecules.

Irradiations were performed at room temperature both in bulk with dry single crystals placed in a sealed vial under argon (Figure S8) or with a single crystal mounted on the pin of a diffractometer's goniometer head, ready to be measured after irradiation. The irradiation wavelength was chosen as 465 nm (same for anthraphane, tail-end irradiation[38]). The results are summarized in Figure 3b. Photopolymerizations turned out to be very fast. Already within 15 min of irradiation at room temperature monomer single crystals smoothly convert into polymer single crystals of **PA2**. The unit cell parameters are minimally affected by the reaction: the *a*-axis lengthens by 0.4%, the *b*-axis shortens by 1.6%, the *c*-axis lengthens by 0.5% and β is the only angle affected, increasing by 5%. These minimal changes are a consequence of the nicely overlapping anthracene pairs, and prevent the crystals from cracking during the reaction. The quality of the crystals after irradiation slightly increased, allowing to model additional solvent molecules in the crystal structure, which had to be masked in the monomer crystal (Figure S20). In the

10.1002/chem.201802513

particular crystal measured, again the main molecule appeared disordered in its orientation: approximately 77% of the molecules had their trimethoxybenzene cores oriented in one direction and 23% in the opposite direction. Polymerization also resulted in visible discoloration of the crystals due to the consumption of the anthracene chromophores.

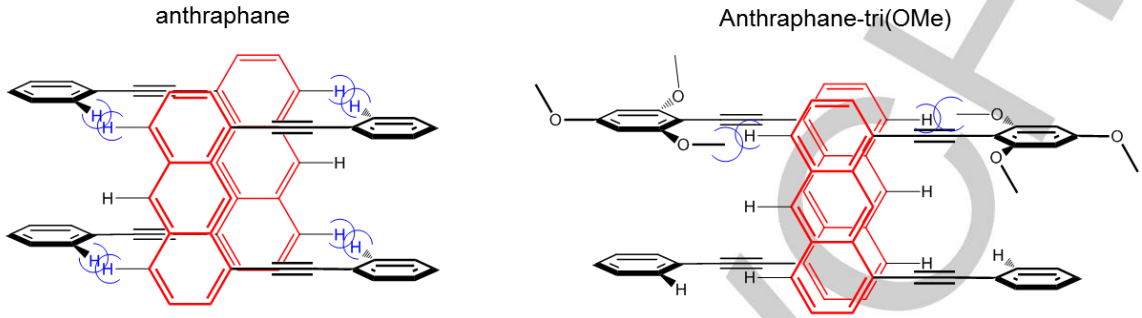

Figure 4. . Schematic offset of the anthracene pairs in crystal structures of anthraphanes **1** (*left*) and **2** (*right*). Substituents at the central benzene cores prevent interpenetration with consequent slipping of the anthracene pairs.

Face indexing shed light into the orientations of the chains in the crystal (Figure 5), showing that they run along the longest dimension of the rhombohedra being typically 180 µm, whereas the layers stack along the shorter dimension of 150 µm. The length of 180 µm would ideally corresponds to linear chains with approximately 150'000 repeat units and molar masses of 136 MDa. We however do not expect having accomplished such outstanding molar masses because of crystal defects and the phenomenon of mosaicity[39,40], which lead to grain boundaries which may or may not interrupt the polymerization reactions. However, we highlight the fact that the formation of this linear polymer is unique to the single crystalline state. If attempted in solution, not only the selectivity towards linear growth would not be ensured due to the monomer's trifunctionality, but also the molecular weights would be much lower, since rigid monomer such as **2** tend to precipitate out of the solution already at the oligomeric state.

The polymer crystals were further characterized by fluorescence spectroscopy (Figure S22), ^{13}C-CP/MAS NMR-, and ATR-FTIR spectroscopy (Figure S24). In the solid-state NMR spectrum of the polymer crystals, the characteristic peaks at 49.2 ppm and 51.6 ppm corresponding to the bridge carbons of the anthracene dimers are clearly visible (Figure S23). Not surprisingly the polymerized crystals are completely insoluble; additional characterization of the polymer would require exfoliation in a suitable solvent which is currently in progress. Preliminary experiments show that exposure to NMP at room temperature breaks down the mother crystals into needles (Figure S28).

[4+4]-Cycloadditions are known to be reversible. Not surprisingly, poly$_{1D}$anthraphane-tri(OMe) **PA2** upon thermal treatment underwent depolymerization as confirmed by both ^{13}C-CP/MAS NMR ATR-FTIR spectroscopy (Figure S23 and S26): heating the crystals under argon at 200°C for 24 h resulted in complete depolymerization but also resulted in loss of crystallinity. The crystals maintained their shapes without turning into powder but showed poor diffraction upon SC-XRD. As expected, irradiation of the depolymerized crystals did not result in repolymerization. Differential scanning calorimetry (DSC), also confirmed the thermal retro-polymerization by showing a typical exotherm appearing above 200°C (Figure S27).

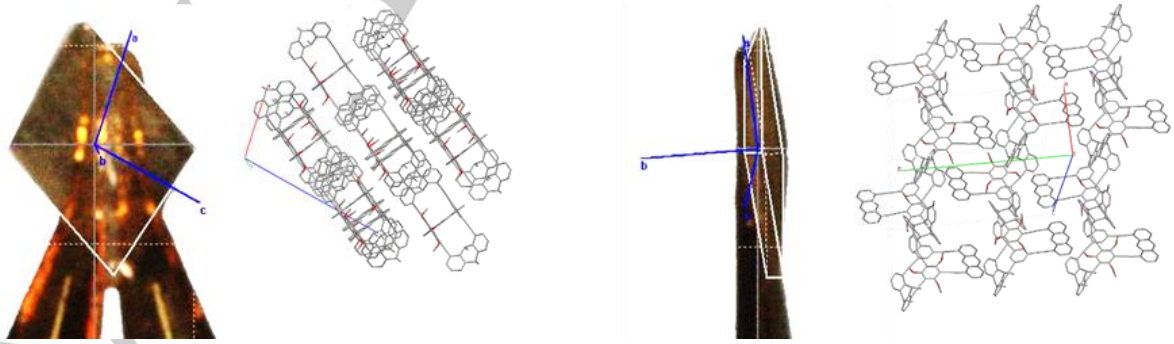

Figure 5. Face indexing of a rhombohedral single crystal mounted on the pin of a goniometer head showing how the polymer chains are oriented within it.

10.1002/chem.201802513

Finally, we turn the attention to the architecture of the polymer **PA2** itself: while it might seem analogous to the polyanthraphane **PA1**, there is a fundamental difference between both polymers. This difference goes beyond the presence of the methoxy functional groups and concerns how the repeat units are connected together in terms of stereochemistry (Figure 6). Anthracenes have two faces, both of which are potentially accessible for stacking and consequent photodimerisation: in the case of polyanthraphane **PA1**, in the crystal structure the two faces engaged in *ftf* stacking are the ones pointing away (*exo*) from the unreacted anthracene unit, resulting in a poly-(*exo*,*exo*)-anthraphane; in the present study however, the stacking faces were the ones pointing towards the unreacted anthracene (*endo*), resulting in a poly-(*endo*,*endo*)-anthraphane-tri(OMe), **PA2**. This isomerism results in chains being approximately 26% thicker in the *exo*,*exo* polymer (≈ 30.1 Å) with respect to the *endo*,*endo* case (≈ 23.8 Å). Consequently the chains are also 20% shorter in the *exo*,*exo* polymer compared to the *endo*,*endo* one.

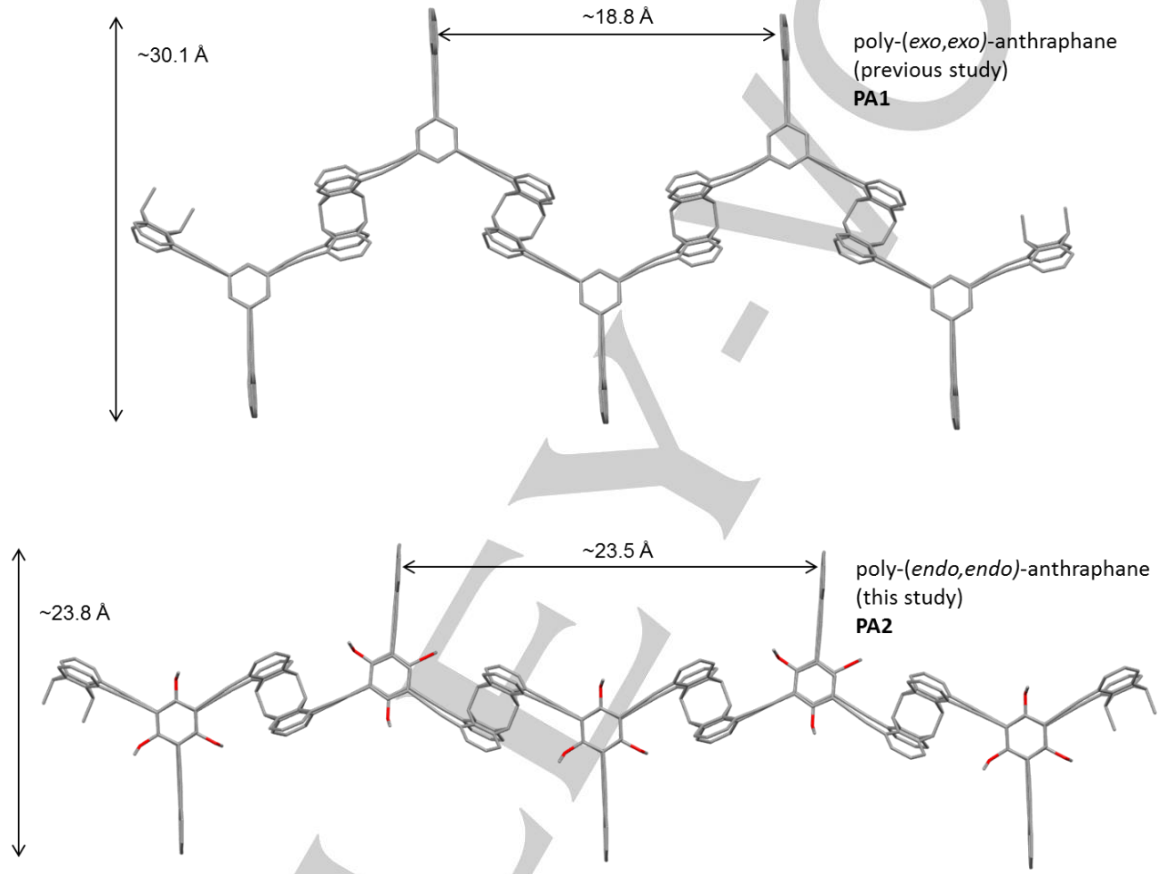

Figure 6. Stereoisomerism in polyanthraphanes affects the molecular structure of the polymer chains. Depending on the stacking preference of anthracene pairs, *exo*,*exo* polymers or *endo*,*endo* polymers were obtained, each with their characteristic molecular dimensions. The reported dimensions account for van der Waals radii.

Conclusions

In conclusion, we synthesized the desymmetrized anthraphane-tri(OMe) **2** using the new building block **6** while keeping the synthetic protocol developed for the original hydrocarbon anthraphane **1** unchanged. Compound **2** was crystallized from different solvents resulting in two new packing motifs, *etf* packing 3 and the photoreactive *etf*/*ftf* packing 5, which add to the previously reported seven packings known for anthraphane. Irradiation of the *etf*/*ftf* packing 5 single crystals resulted in a SCSC linear photopolymerization via [4+4]-cycloaddition of *ftf*-stacked anthracenes, affording single crystals of polyanthraphane-tri(OMe), **PA2**, the second polyanthraphane reported so far. We found that substitution with methoxy groups at the central benzene core of the cyclophane, can sterically force the anthracene pairs into a near-perfect stacking, resulting in a very smooth and fast polymerization process, with minimal changes in the unit cell parameters of the crystals. Depolymerization by retro-[4+4]-cycloaddition was found to be initiated at temperatures above 200°C. This study also highlights an unprecedented case of isomerism characteristic of polyanthraphanes, which can result in *endo*,*endo* or *exo*,*exo* configured polymers depending on which face of the anthracene moieties the dimerisation reaction takes place. We would expect

10.1002/chem.201802513

such differences to impact for instance the solubility of the chains, where in the *exo*,*exo* polymer the free anthracene units would be more exposed to solvent interaction and have more degrees of freedom. *Endo*,*exo* or *exo*,*endo* chains are still elusive, but would also of course widen the architectural palette of polyanthraphanes. Apart from that, such structural differences might be of interest for construction of nanostructures with well-defined molecular dimensions involving the still unreacted anthracene units provided in fixed relative distances and orientations. Last but not least, we note that crystal packing effects do not seem to be sufficient to clearly steer the orientation of the trimethoxybenzenes units of **2** in a defined way. Being able to control the orientation would open access to piezoelectric polymers having chains with specific permanent dipole moments[41,42].

Experimental Section

Materials and Methods

All reactions were carried out under nitrogen by using standard Schlenk techniques and dry solvents unless otherwise noted. Dry diethyl ether, dry methanol, dry DMI and dry toluene were purchased over molecular sieves from Acros and used directly. Diisopropyl amine was dried by passing it over a column of activated neutral aluminum oxide. $Pd(PPh_3)_4$ catalyst was freshly prepared and stored in a glove-box in the dark under N_2 at room temperature. All reagents were purchased from Acros, Aldrich or TCI, and used without further purification. Column chromatography for purification of the products was performed by using Merck silica gel Si60 (particle size 40-63 µm). NMR was recorded on a Bruker AVANCE (^{1}H: 300 MHz, ^{13}C: 75 MHz) at room temperature. The signal from the solvents was used as internal standard for chemical shift (^{1}H: δ = 7.26 ppm, ^{13}C: δ = 77.16 ppm for chloroform, ^{1}H: δ = 6.00 ppm, ^{13}C: δ = 73.78 ppm for 1,1,2,2-tetrachloroethane, ^{19}F: δ = -164.9 ppm for hexafluorobenzene). High resolution mass spectroscopy (HRMS) analyses were performed by the MS-service of the Laboratory for Organic Chemistry at ETH Zurich with spectrometers (ESI- and MALDI-ICR-FTMS: IonSpec Ultima Instrument).

Synthetic Procedures

1,3,5-trifluoro-2,4,6-triiodobenzene 3

Periodic acid (5.13 g, 22.5 mmol, 1.50 eq) was suspended in 35 mL sulphuric acid at 0°C. Finely ground potassium iodide (11.2 g, 67.6 mmol, 4.50 eq) was added in portions over 5 min during which time iodine vapours evolved. 1,3,5-Trifluorobenzene (1.56 mL, 15.1 mmol, 1.00 eq) was then added by syringe at 0°C and the reaction mixture was then heated to 70°C for 5 h, during which time additional sulphuric acid can be added for better stirring. After cooling to room temperature, the reaction mixture was poured into 350 g crushed ice. 200 mL diethyl ether were added and the layers separated. The organic layer was washed once with 150 mL of a 15% solution of sodium thiosulfate, once with 150 mL water, dried over $MgSO_4$ and concentrated to dryness. The residue was purified by sublimation: the temperature was kept at 50°C (p = 0.04 mbar) for 1 h, during which time a brown layer coated the cold finger, then it was increased to 110°C to allow sublimation of the product. Compound **3** was obtained as a white crystalline solid (7.60 g, 14.9 mmol, 97%). R_f (hexane): 0.6, Mp: 156-158 °C. ^{13}C-NMR (75.5 MHz, $CDCl_3$) δ/ppm: 162.4 (dt, *J* = 243.5, 7.8 Hz), 63.9 (ddd, *J* = 34.9, 34.1, 3.9 Hz). ^{19}F-NMR (282.5 MHz, $CDCl_3$) δ/ppm: 68.83. HRMS (FT-MALDI): m/z calcd for $C_{14}H_{13}O_2$ $[M-H]^+$: 213.0910; found: 213.0909.

1,3,5-triiodo-2,4,6-trimethoxybenzene 4

Sodium hydride (0.94 g, 23.5 mmol, 6 eq, 60% dispersion in mineral oil) was suspended in 10 mL dry diethyl ether in a 100 mL Schlenk flask. MeOH (1.00 mL, 23.5 mmol, 6 eq) diluted in 10 mL dry diethyl ether was slowly added to the hydride under vigorous stirring. The reaction mixture was then stirred at room temperature for 1 h until no more hydrogen evolution was detectable. The volatiles were removed by a stream of nitrogen and the residue was dried on HV for 10 min. 20 mL dry DMI were then added to the residue and to the resulting suspension 1,3,5-trifluoro-2,4,6-triiodobenzene **3** (2.00 g, 3.92 mmol, 1 eq) was added in small portions over 30 min under vigorous stirring (caution: some foaming during this exothermic reaction is possible). The obtained orange suspension was stirred overnight at room temperature and then poured into 80 mL saturated $NaHCO_3$ solution. The white precipitate was collected by filtration and washed with water until the pH of the filtrate resulted neutral. Recrystallization from boiling methanol afforded compound **4** as white needles (1.56 g, 2.86 mmol, 73%). R_f (30% EtOAc in hexane): 0.72, Mp: 176-178°C. ^{1}H-NMR (300 MHz, $CDCl_3$) δ/ppm: 3.86 (s, 9H). ^{13}C-NMR (75.5 MHz, $CDCl_3$) δ/ppm: 161.5, 82.8, 60.9. HRMS (FT-MALDI): m/z calcd for $C_9H_9I_3O_3$ $[M-H]^+$: 545.7680; found: 545.7680.

((2,4,6-trimethoxybenzene-1,3,5-triyl)tris(ethyne-2,1-diyl))tris(trimethylsilane) 5

1,3,5-triiodo-2,4,6-trimethoxybenzene **4** (180 mg, 0.33 mmol, 1.00 eq) was placed in a dry 20 mL Schlenk tube along with catalyst $Pd(OAc)_2$ (4.00 mg, 0.02 mmol, 0.05 eq), co-catalyst CuI (3.00 mg, 0.02 mmol, 0.05 eq) and ligand tri-tert-butylphosphonium tetrafluoroborate (9.00 mg, 0.03 mmol, 0.10 eq). In a separate Schlenk tube, 10 mL dry diisopropylamine were degassed by four cycles of freeze-pump-thaw and then added by syringe to the reactants. Trimethylsilylacetylene (0.20 mL, 1.65 mmol, 5 eq) was added and the reaction mixture was sealed and heated to 65°C for 48 h under an argon atmosphere. Formation of a beige precipitate indicated the start of the reaction. After cooling to room temperature, the reaction mixture was filtered through a celite pad and concentrated to dryness. Separation by column chromatography (3% EtOAc in hexane) afforded the title compound **5** as a yellowish solid of purities high enough for the next step (98 mg, 0.21 mmol, 65%). R_f: 0.37, Mp: 82-84°C. ^{1}H-NMR (300 MHz, $CDCl_3$) δ/ppm: 4.02 (s, 9H), 0.24 (s, 27H). ^{13}C-NMR (75.5 MHz, $CDCl_3$) δ/ppm: 163.5, 108.3, 103.5, 96.1, 59.3, 0.0. HRMS (FT-MALDI): m/z calcd for $C_{24}H_{36}O_3Si_3$ $[M]^+$: 456.1972; found: 456.1970.

1,3,5-triethynyl-2,4,6-trimethoxybenzene 6

Compound **5** (0.20 g, 0.44 mmol, 1 eq) was dissolved in a solvent mixture of 5 mL THF and 2 mL MeOH. Potassium carbonate (7.00 mg, 0.05 mmol, 0.12 eq) and 0.5 mL H_2O were added and the reaction mixture was stirred at room temperature for 16 h. After removal of the solvents in vacuo, 5 mL H_2O were added to the residue, which was then extracted with DCM (3 x 15 mL). The combined organic phases were dried over $MgSO_4$, concentrated and subjected to flash column chromatography (10% EtOAc in hexane) to afford the title compound **6** as a white solid (97 mg, 0.40 mmol, 92%). The product must be stored in the fridge protected from light and under nitrogen (decomposition is characterised by a blue-coloration and insolubility in organic solvents). R_f: 0.24 , Mp: 125-127°C. ^{1}H-NMR (300 MHz, $CDCl_3$) δ/ppm: 4.06 (s, 9H), 3.46 (s, 3H). ^{13}C-NMR (75.5 MHz, $CDCl_3$) δ/ppm: 165.7, 106.8, 85.8, 74.8, 61.7. HRMS (FT-MALDI): m/z calcd for $C_{15}H_{13}O_3$ $[M-H]^+$: 214.0859; found: 214.0870.

Anthracene-1,8-ditriflate 7

Compound **7** was synthesised according to the literature procedure[4]. ^{1}H-NMR (300 MHz, $CDCl_3$) δ/ppm: 8.90 (s, 1H), 8.61 (s, 1H), 8.07 (d, *J* = 7.8 Hz, 2H); 7.62-7.50 (m, 4H). ^{19}F-NMR (282.5 MHz, $CDCl_3$) δ/ppm: -76.36. ^{13}C-NMR (75.5 MHz, $CDCl_3$) δ/ppm: 145.7, 133.1, 128.9, 127.9, 125.6, 125.4, 118.9 (q, J_{CF} = 320.3 Hz), 118.4, 114.1. HRMS (FT-MALDI): m/z calcd for $C_{16}H_8F_6O_6S_2$ $[M]^+$: 473.9661; found: 473.9661. Mp: 111°C.

(benzene-1,3,5-triyltris(ethyne-2,1-diyl))tris(anthracene-8,1-diyl) tris(trifluoromethanesulfonate) 8

Compound **8** was synthesised according to the literature procedure[4]. ^{1}H-NMR (300 MHz, $C_2D_2Cl_4$) δ/ppm: 9.36 (s, 1H), 8.61 (s, 1H), 8.19 (s, 1H), 8.16-8.08 (m, 2H), 7.98 (d, *J* = 7.1 Hz, 1H), 7.63 (dd, *J* = 8.6 Hz, 7.0 Hz, 1H), 7.58-7.50 (m, 2H). ^{13}C-NMR (75.5 MHz, $C_2D_2Cl_4$) δ/ppm: 145.8, 134.5, 132.6, 131.8, 131.61, 131.57, 129.0, 128.6, 127.5, 126.0, 125.0, 124.3, 124.0, 121.3, 118.9, 118.7 (q, J_{CF} = 321.0 Hz), 117.3, 94.0, 88.0. ^{19}F-NMR (282.5 MHz, $C_2D_2Cl_4$) δ/ppm: -76.65. HRMS (FT-MALDI): m/z calcd for $C_{57}H_{27}F_9O_9S_3$ $[M]^+$: 1122.0668; found: 1122.0673. Mp: decomposes above 270°C.

Anthraphane-tri(OMe) 2

Precursor **8** (640 mg, 0.57 mmol, 1.00 eq) was suspended in 380 mL dry toluene (1.50 mM) with compound **6** (137 mg, 0.57 mmol, 1.00 eq) and dry triethylamine (15.8 mL, 114 mmol, 200 eq). The reaction mixture was degassed by cooling it to -80°C with an acetone-dry ice bath and then performing five cycles of vacuum (10 min) and nitrogen backfilling. $Pd(PPh_3)_4$ (197 mg, 0.17 mmol, 0.30 eq) was added with N_2 counter-flow and the suspension was degassed twice again and backfilled with argon after the last cycle. After warming to room temperature, the reaction mixture was put in a preheated bath at 80°C and stirred in the dark under argon for 5 d. After cooling to room temperature, the reaction mixture was filtered and the filtrate was concentrated to dryness. The brownish residue was washed with MeOH to obtain a beige solid, which was collected by filtration and rinsed with more MeOH until the filtrate resulted colourless. The beige solid was then dissolved in tetrachloroethane and slowly precipitated with MeOH to obtain the pure product **2** as a pale yellow solid (203 mg, 0.22 mmol, 39%). The product can be recrystallized from dioxane to obtain yellow needles. R_f (20%EtOAc in hexane): 0.27 (blue fluorescence with λ = 366 nm), Mp: decomposes above 280°C. ^{1}H-NMR (300 MHz, $C_2D_2Cl_4$) δ/ppm: 9.54 (s, 3H), 8.56 (s, 3H), 8.11 (d, *J* = 8.6 Hz, 6H), 7.90-7.80 (m, 6H), 7.77 (s, 3H), 7.60-7.50 (m, 6H), 4.14 (s, 9H). ^{13}C-NMR (75.5 MHz, $C_2D_2Cl_4$) δ/ppm: 164.22, 134.10, 131.68, 131.44, 131.41, 131.29, 130.16, 130.11, 129.29, 128.97, 127.30, 125.30, 125.08, 123.93, 123.85, 121.31, 120.62, 107.41, 94.64, 92.09, 88.27, 85.42, 62.05. HRMS (FT-MALDI): m/z calcd for $C_{69}H_{36}O_3$ $[M]^+$: 912.2659; found: 912.2657.

Crystallization Procedure

For the screening crystallization procedure, 3 mg anthraphane were suspended in 0.5 ml solvent inside a clean glass vial equipped with a screw cap lined with Teflon. The suspension was briefly degassed by purging it with argon and subsequently sealed and heated close to the boiling point of the solvent in a sand bath. If a clear solution was not obtained, 0.1 mL solvent were added and the degassing/heating process repeated. Once a clear solution was obtained, the vial was controlled-cooled to room temperature over 24 h, by using a PID controller coupled to the heating plate (Figure S6). The crystallization process was carried out in a vibration-free environment and exposure to light was avoided as much as possible. For the preparation of the monomer crystals of *etf*/*ftf* packing 5, 15 mg of **2** were typically crystallized from 1.5 mL nitrobenzene.

Topochemical single-crystal-to-single-crystal (SCSC) reactions

For the SCSC polymerization, an *in-house* built cylindrical photoreactor was used (Figure S10) equipped with 16 high power LEDs (465 nm) with a nominal dissipation power of 16 x 2.8 W = 44.8 W and a luminous flux of approximately 30 Lumen per LED at I = 400 mA. The single crystals were either irradiated on the pin of a goniometer head after being mounted or in bulk. The pin with the crystal was put in the middle of the reactor and to regulate the temperature of irradiation (0°C or 20°C), a cooler from an X-ray diffractometer was used, having the nitrogen stream just above the pin. For bulk irradiation, the nitrobenzene mother liquor was removed from a freshly crystallized batch and the crystals were rinsed three times with methanol, then dried with a stream of nitrogen (the single crystals perfectly withstand the washing procedure and can be stored dry over weeks without losing their crystallinity). The single crystals were placed in a sealed vial previously purged with argon and put in the LED reactor; every once in a while the vial was shaken and turned in order to homogeneously irradiate the mass of crystals.

Supporting Information

NMR data and synthetic procedures to compound **2**. Details on crystallization procedure, polymorphism and experimental setup for SCSC reactions. Crystallographic data for every co-crystal, with optical micrographs and additional information on the structures. ATR-FTIR spectra and UV/Vis emission spectra of the monomer and polymer crystals. ^{13}CP-MAS NMR data. DSC measurements.

Acknowledgements

We thank Dr. Kirill Feldman and Prof. Jan Vermant (Laboratory of Polymer Technology, ETH Zürich) for access to the optical microscopy equipment; many thanks go to Dr. Thomas Schweizer (Institute of Polymer Chemistry, ETH Zürich) for providing the PID-controller and crystallization apparatus and for building the LED-photoreactor. Many thanks to Michael Solar (Laboratory of Inorganic Chemistry, Small Molecule Crystallography Center, ETH Zurich) for measuring the single crystals. The help of Dr. René Verel (Laboratory of Inorganic Chemistry, ETH Zürich) for the solid-state NMR measurements is greatly acknowledged.

Conflict of Interest

The authors declare no conflict of interest.

Keywords: single-crystal-to-single-crystal polymerization• anthracene • [4+4]-cycloaddition • cyclophane • crystal engineering

[1] B. M. D. Cohen, G. M. J. Schmidt, *J. Chem. Soc.* **1964**, 1996–2000.
[2] M. D. Cohen, G. M. J. Schmidt, F. I. Sonntag, *J. Chem. Soc.* **1964**, 2000–2013.
[3] G. M. J. Schmidt, *Solid State Photochemistry*, Verlag Chemie, Weinheim, **1976**.
[4] M. Servalli, N. Trapp, M. Wörle, F. G. Klärner, *J. Org. Chem.* **2016**, *81*, 2572–2580.
[5] H. Bouas-Laurent, J.-P. Desvergne, A. Castellan, R. Lapouyade, *Chem. Soc. Rev.* **2000**, *29*, 43–55.
[6] H. Bouas-Laurent, J.-P. Desvergne, A. Castellan, R. Lapouyade, *Chem. Soc. Rev.* **2001**, *30*, 248–263.
[7] I. Zouev, D. Cao, T. V. Sreevidya, M. Telzhensky, M. Botoshansky, M. Kaftory, *CrystEngComm* **2011**, *13*, 4376–4381.
[8] J. Ferguson, A. W.-H. Mau, *Mol. Phys.* **1974**, *27*, 377–387.
[9] A. D. Schlüter, *Adv. Mater.* **1991**, *3*, 282–291.
[10] Y. C. Teo, H. W. H. Lai, Y. Xia, *Chem. Eur. J.* **2017**, *23*, 14101–14112.
[11] J. Sakamoto, J. Van Heijst, O. Lukin, A. D. Schlüter, *Angew. Chem. Int. Ed.* **2009**, *48*, 1030–1069.
[12] M. Servalli, *Chimia* **2017**, *71*, 359-368.
[13] M. Servalli, H. C. Öttinger, A. D. Schlüter, *Phys. Today* **2018**, *71*, 40.
[14] M. Servalli, N. Trapp, M. Solar, A. D. Schlüter, *Cryst. Growth Des.* **2017**, *17*, 3419-3432.

10.1002/chem.201802513

[15] M. Servalli, M. Solar, N. Trapp, M. Wörle, A. D. Schlüter, *Cryst. Growth Des.* **2017**, *17*, 6510−6522.
[16] M. Hasegawa, Y. Suzuki, *J. Polym. Sci. Part B Polym. Lett.* **1967**, *5*, 813–815.
[17] G. Wegner, *Zeitschrift für Naturforsch.* **1969**, *24 B*, 824–832.
[18] A. Matsumoto, T. Matsumura, S. Aoki, *Macromolecules* **1996**, *29*, 423–432.
[19] T. Itoh, S. Nomura, T. Uno, *Angew. Chem. Int. Ed.* **2002**, *41*, 4306–4309.
[20] M. Li, A. D. Schlüter, J. Sakamoto, *J. Am. Chem. Soc.* **2012**, *134*, 11721–11725.
[21] S. Nomura, T. Itoh, H. Nakasho, T. Uno, M. Kubo, K. Sada, K. Inoue, M. Miyata, *J. Am. Chem. Soc.* **2004**, *126*, 2035–2041.
[22] M. Zhu, L. Yin, Y. Zhou, H. Wu, L. Zhu, *Macromolecules* **2018**, *51*, 746–754.
[23] S. L. Huang, T. S. A. Hor, G. X. Jin, *Coord. Chem. Rev.* **2017**, *346*, 112–122.
[24] K. Novak, V. Enkelmann, G. Wegner, K. B. Wagener, *Angew. Chem. Int. Ed.* **1993**, *32*, 1614–1616.
[25] L. Dou, Y. Zheng, X. Shen, G. Wu, K. Fields, W.-C. Hsu, H. Zhou, Y. Yang, F. Wudl, *Science* **2014**, *343*, 272–277.
[26] W. L. Xu, M. D. Smith, J. A. Krause, A. B. Greytak, S. Ma, C. M. Read, L. S. Shimizu, *Cryst. Growth Des.* **2014**, *14*, 993–1002.
[27] Y.-Q. Lan, W.-W. He, S.-L. Li, *Inorg. Chem. Front.* **2018**, *5*, 279–300.
[28] J. W. Lauher, F. W. Fowler, N. S. Goroff, *Acc. Chem. Res.* **2008**, *41*, 1215–1229.
[29] A. Matsumoto, T. Tanaka, T. Tsubouchi, K. Tashiro, S. Saragai, S. Nakamoto, *J. Am. Chem. Soc.* **2002**, *124*, 8891–8902.
[30] G. Hennrich, *Tetrahedron* **2004**, *60*, 9871–9876.
[31] G. Hennrich, I. Asselberghs, K. Clays, A. Persoons, *J. Org. Chem.* **2004**, *69*, 5077–5081.
[32] H. H. Wenk, W. Sander, *Eur. J. Org. Chem* **2002**, 3927–3935.
[33] M. Schilz, H. Plenio, *J. Org. Chem.* **2012**, *77*, 2798–2807.
[34] G. C. Fu, *Acc. Chem. Res.* **2008**, *41*, 1555–1564.
[35] G. M. J. Schmidt, *Pure Appl. Chem.* **1971**, *27*, 647–678.
[36] G. R. Desiraju, J. J. Vittal, A. Ramanan, *Crystal Engineering: A Textbook*, World Scientific Publishing Company, **2011**.
[37] G. R. Desiraju, *J. Am. Chem. Soc.* **2013**, *135*, 9952–9967.
[38] V. Enkelmann, *Mol. Cryst. Liq. Cryst. Sci. Technol.* **1998**, *313*, 15–23.
[39] J. M. Thomas, *CrystEngComm* **2011**, *13*, 4304.
[40] J. O. Williams, J. M. Thomas, *Mol. Cryst. Liq. Cryst.* **1972**, *16*, 371–375.
[41] J. E. Mark, P. J. Flory, *J. Am. Chem. Soc.* **1966**, *88*, 3702–3707.
[42] W. Heywang, K. Lubitz, W. Wersing, *Piezoelectricity*, Springer, Berlin, Heidelberg, **2008**.

10.1002/chem.201802513

WILEY-VCH

Entry for the Table of Contents (Please choose one layout)

Layout 2:

FULL PAPER

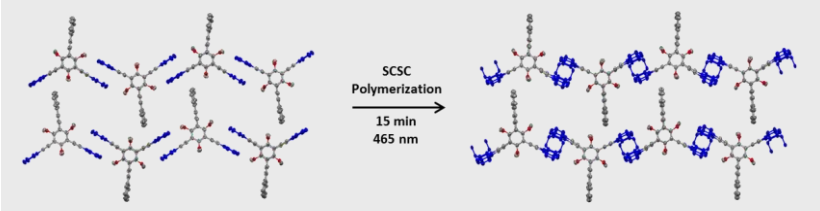

Text for Table of Contents

Marco Servalli, Nils Trapp, A. Dieter Schlüter*

Page No. – Page No.

Single-Crystal-to-Single-Crystal (SCSC) Linear Polymerization of a Desymmetrized Anthraphane